https://doi.org/10.5194/egusphere-2026-1301
Preprint. Discussion started: 7 April 2026

A process-based perspective on Antarctic sea ice regimes using objective data mining

Jinfei Wang[1,2], Maike Sonnewald[3,4,5], Noé Pirlet[2], François Massonnet[2], Hugues Goosse[2], Dake Chen[1], Qinghua Yang[1]

[1]School of Atmospheric Sciences, Sun Yat-sen University, and Southern Marine Science and Engineering Guangdong Laboratory (Zhuhai), Zhuhai, 519082, China
[2]Earth and Climate Center, Earth and Life Institute, Université catholique de Louvain, Louvain-la-Neuve, 1348, Belgium
[3]Department of Computer Science, University of California, Davis, 95616, USA
[4]University of Washington, Seattle, 98195, USA
[5]NOAA/Geophysical Fluid Dynamics Laboratory, Princeton, 08540, USA

Correspondence to: Qinghua Yang (yangqh25@mail.sysu.edu.cn)

Abstract. Antarctic sea ice has undergone unprecedented changes in recent years, marked by a stepwise shift from long-term expansion to rapid decline since 2016. Yet the underlying processes remain poorly understood due to the complex interplay of dynamic and thermodynamic drivers. Using an ascendant data mining framework, we objectively classify sea ice into distinct process-based regimes during the growth season in the NEMO-SI^3 model. Six robust regimes with unique combinations of dynamic and thermodynamic drivers are identified. We reveal that a coastal regime, characterized by strong dynamic divergence and compensating thermodynamic ice growth, has experienced significant area loss since 1979, accelerating after 2016, potentially reflecting weakened new ice formation. Meanwhile, sea ice extent anomalies closely correlate with both the coastal and a pack ice regime, highlighting their dominant role in overall sea ice variability. By capturing physically consistent sea ice regimes, our work offers a new process-based perspective for understanding Antarctic sea ice variability and its unprecedented recent changes.

1 Introduction

Antarctic sea ice is a key component of the global climate system, substantially influencing ocean-atmosphere interactions (Søren et al., 2011; Ayres et al., 2022), ice-shelf stability (Massom et al., 2018; Kusahara et al., 2023), global ocean circulation (Li et al., 2023; van Westen et al., 2024), and polar ecosystems (Lim et al., 2023; Swadling et al., 2023). Over the past 45 years, total Antarctic sea ice extent (SIE) first exhibited a gradual increase until 2015 (Parkinson, 2019), and then displayed a sharp decline followed by record-low austral summer minimums in 2017, 2022 and 2023 (Turner and Comiso, 2017; Wang et al., 2022, 2024). Meanwhile, the winter maximum SIE reached its lowest level in 2023 (Jena et al., 2024) and second lowest in 2024. These substantial post-2016 decreases in Antarctic SIE highlight the need to uncover the mechanisms driving those changes to better interpret extreme states and to improve projections of the future evolution of sea-ice. However, there is currently no consensus on whether these changes are primarily driven by thermodynamic or dynamic

https://doi.org/10.5194/egusphere-2026-1301
Preprint. Discussion started: 7 April 2026

processes (Meehl et al., 2019; Zhang et al., 2022; Schroeter et al., 2023; Espinosa et al., 2024; Himmich et al., 2024). To address this uncertainty, we conduct a process-based analysis of sea ice variability across different spatial and temporal scales and develop a regime-identification framework to diagnose the physical drivers.

Dividing Antarctic sea ice into specific sub-regions allows for a unified analysis of sea ice regimes within areas where sea ice characteristics are similar, while also facilitating more precise comparisons across these sub-regions. Geographical divisions (e.g. the Weddell Sea, the Indian Ocean, the western Pacific Ocean, the Ross Sea, and the Bellingshausen-Amundsen Seas) have provided valuable insights. The regionality of Antarctic sea ice is highly pronounced, with for instance generally opposing trends between the Ross Sea and the Bellingshausen-Amundsen Seas (Liu et al., 2004; Comiso et al., 2017). However, this division may not be suitable for all research contexts, as has been demonstrated for the present ocean circulation (Sonnewald et al., 2023), and could overlook coherent regimes shaped by underlying physical processes or variability patterns across sectors. Alternative approaches, such as those based on sea ice variability (Raphael and Hobbs, 2014), provide an additional perspective to the geographical framework.

New advances in data mining techniques, particularly clustering algorithms, offer innovative solutions to the challenge of objectively describing sea ice regimes. In complement to analyses based on geographical divisions, these methods can enhance our understanding by identifying spatial patterns with consistent dynamic and thermodynamic characteristics, thereby offering a process-based view of Antarctic sea ice variability (Sonnewald et al., 2023). By applying appropriate clustering methods, it is possible to explore nonlinear and complex datasets and reveal underlying patterns that are often obscured by traditional approaches. Unsupervised clustering techniques have proven effective in analyzing the Antarctic processes. For example, Wachter et al. (2021) used the “dkmeans” clustering to describe variability in annual cycles of sea ice concentration and their spatial distribution. Gaussian mixture modeling has been employed to objectively identify the location of regimes around the Antarctic margins (Sohail and Zika, 2024). Moreover, “k-means” clustering has been applied to sea ice data simulations to separate the marginal ice zone from the inner ice pack (Day et al., 2024). Despite these advances, these methods generally require the number of clusters to be specified and assume clusters have regular shapes (e.g., spherical or elliptical). In contrast, our study employs the DBSCAN (Density-Based Spatial Clustering of Applications with Noise) clustering algorithm, combined with UMAP (Uniform Manifold Approximation and Projection) manifold methodology and uncertainty estimates, to identify arbitrarily shaped clusters without predefining the number of clusters, described further below.

The way we apply our machine learning framework is designed to transform traditional empirical leading order analysis into an objective approach. By incorporating sea ice budget components into clustering analysis, we can capture key processes such as sea ice formation, melting, dynamic transport and redistribution, and provide deeper insights in understanding the

https://doi.org/10.5194/egusphere-2026-1301
Preprint. Discussion started: 7 April 2026

mechanisms driving sea ice change. This process-based methodology enables an objective analysis of the sea-ice mass balance, offering unprecedented ability to quantify Antarctic sea-ice changes and their recent shifts.

It is important to distinguish between the 'regimes' defined here (i.e., characteristic modes of sea ice variability associated with specific dynamic and thermodynamic processes) and the 'regime shift' concept discussed in recent studies, which suggests that Antarctic sea ice has entered a new state marked by more extreme events (Raphael and Handcock, 2022; Purich and Doddridge, 2023; Schroeter et al., 2023; Hobbs et al., 2024). While these studies primarily identify shifts in the mean sea ice state or increased sea ice variability over the past decades, our work focuses on uncovering spatially distinct sea ice regimes at a given time. However, the temporal 'regime shift' may result from changes in the location and magnitude of our spatially defined regimes.

Our framework is the Native Emergent Manifold Interrogation (NEMI) method (Sonnewald, 2023), an ascendant data mining workflow designed for noisy and nonlinear datasets, on Antarctic sea ice mass balance components simulated by an ocean–sea ice model. The NEMI method is particularly effective at strengthening associations among the input variables and quantifying the uncertainties of the clustering results (Sonnewald, 2023; Jenniges et al., 2025). By scaling, embedding, and clustering the sea ice budget components from the NEMO-SI³ ocean–sea ice coupled model during the growth seasons from 1979 to 2023, we aim to objectively and stably identify dominant sea ice regimes based on their dynamic and thermodynamic behaviors. In addition, the NEMI workflow allows for the estimation of uncertainty, providing stability measures for the identified regimes. The growth season was chosen as it represents a critical period when sea ice formation and associated processes are most active, allowing us to have a first glimpse of how sea ice regimes are determined by dynamic and thermodynamic processes. In contrast, during the melt season, the clustering results show decreased stability and reduced interpretability (Figure S1-S3), consistent with previous findings that dominant processes are different during growing and melting seasons, and models generally perform less reliably for Antarctic sea ice in this period (Eayrs et al., 2019; Goosse et al., 2023).

2 Methods

2.1 NEMO-SI³ configuration and evaluation

Focusing on the Antarctic sea ice budget components at a circumpolar scale, we use the ocean-sea ice model NEMO-SI³ v4.2.0 in a regional Southern Ocean configuration with a 1/4° (~12 km) resolution. The SI³ (Sea Ice modelling Integrated Initiative), is a dynamic-thermodynamic continuum sea ice model (Rousset et al., 2015), directly integrated on the NEMO (Nucleus for European Modelling of the Ocean) ocean grid (Madec et al., 2024). The eANT025 configuration includes the sea ice region, the Southern Ocean, ice shelves, and has a single boundary at 30 °S. The settings, along with the atmospheric (ERA5) (Hersbach et al., 2020) and oceanic (ORAS5) (Zuo et al., 2019) forcings, align with those described by Pirlet et al.

https://doi.org/10.5194/egusphere-2026-1301
Preprint. Discussion started: 7 April 2026

(2025), with the exception that no correction for snow precipitation was necessary for this study. Based on the configuration, we conducted a simulation for the period 1979-2023, initialized from rest using ocean temperature and salinity from the WOA2018 climatology (World Ocean Atlas 2018) (Locarnini et al., 2018; Zweng et al., 2019).

The modeled climatological (average over 1981-2010) sea ice concentration (SIC) and sea ice thickness (SIT) fields have been evaluated against SIC observations from the National Snow and Ice Data Center (NSIDC) and SIT reanalyses from the Global Ice-Ocean Modeling and Assimilation System (GIOMAS) (Figure S4). The 25 km monthly SIC observations are based on passive microwave measurements from the Nimbus-7 SMMR and DMSP SSM/I-SSMIS instruments that are processed with the NASA Team algorithm (DiGirolamo et al., 2022). The monthly GIOMAS SIT reanalyses are based on the results of the global Parallel Ocean and Sea Ice Model (POIM) with data assimilation capabilities (Zhang and Rothrock, 2003). Our model simulates a climatological SIC distribution comparable to observations during the growth season (Figure S4a-b), despite some underestimations in the Weddell and Amundsen Seas, and overestimations elsewhere (Figure S4c). As for SIT simulations, our model generally underestimates SIT compared with GIOMAS. However, it effectively captures the thick ice in the western Weddell Sea and along the coast of Amundsen Sea as GIOMAS.

As our study focuses on the growth season (defined here as March-September), we also analyze the spatial correlation between observed and modeled SIC (Figure S5a), averaged over March–September from 1979 to 2023. The map reveals a significant mean correlation of 0.69. Our model captures the slight increase in SIE before 2016 and the sharp decrease afterward, showing a significant correlation of 0.68 from 1979 to 2023 (Figure S5b). Overall, the model is adequate to provide sea ice budget components during the growth seasons.

2.2 Sea ice mass balance components

The sea ice mass balance in the NEMO-SI^3 model is represented by the following equation:

$$vfx_{ice} = \left[vfx_{bog} + vfx_{bom} + vfx_{sum} + vfx_{sni}\right] + \left[vfx_{opw} + vfx_{lam}\right] + \left[vfx_{trp} + vfx_{dyn}\right] + vfx_{pnd} + vfx_{sub} + vfx_{suberr} + vfx_{res} \quad (1)$$

The definition of each component is introduced in Table 1. For the growth season analysis, we focus on the primary budget components as data input. We refer to the sum of vfx_{bog}, vfx_{bom}, vfx_{sum}, vfx_{sni} as "vertical thermodynamics", to the sum of vfx_{opw} and vfx_{lam} as "horizontal thermodynamics", and to the sum of vfx_{trp} and vfx_{dyn} as "dynamics". Although most thermodynamic processes are vertical in the real world, vfx_{opw} and vfx_{lam} are categorized as "horizontal thermodynamics" due to their spatial redistribution effects at the ice–open water boundary from the model's perspective, in contrast to purely vertical fluxes such as surface/basal growth/melt. The remaining components are excluded from the

https://doi.org/10.5194/egusphere-2026-1301
Preprint. Discussion started: 7 April 2026

analysis since their magnitudes are on average 1-2 orders smaller than the smallest values of the former components and they have little impact on the clustering result.

Table 1. Definitions of the sea ice mass budget components in the NEMO-SI^3 model (Unit: kg m^{-2} s^{-1}).

	Mass budgets	Definition
	vfx_{ice}	Sea ice mass flux from ice melt/growth
Vertical thermodynamics	vfx_{bog}	Ice bottom growth
	vfx_{bom}	Ice bottom melt
	vfx_{sum}	Ice surface melt
	vfx_{sni}	Snow-ice formation
Horizontal thermodynamics	vfx_{opw}	Ice growth in open water
	vfx_{lam}	Ice lateral melt
Dynamics	vfx_{trp}	Ice mass transport
	vfx_{dyn}	Ice dynamics (ridging)
	vfx_{pnd}	Ice melt ponds
	vfx_{sub}	Ice sublimation
	vfx_{suberr}	Unbalance in sublimation
	vfx_{res}	Undiagnosed processes

2.3 NEMI methodology

The Native Emergent Manifold Interrogation (NEMI) method is applied on Antarctic sea ice budget components. NEMI is an ascendant data mining workflow designed for the noisy and nonlinear datasets, common in Earth science. Through applying a manifold methodology that maps the underlying relationships within the data, NEMI is able to strengthen associations and simplify the covariance structures within the datasets. This is achieved by minimizing an objective function that can be adjusted towards either local or global properties in the data. Once the data is mapped onto this lower-dimensional manifold, referred to as an embedding, a suitable clustering method is used to highlight areas of interest. To ensure the robustness of the results, NEMI incorporates an ensemble technique that assesses the sensitivity of the results to stochastic perturbations. Each cluster is sorted within individual ensemble members and then compared across all ensemble results. External validation through visual inspection as well as statistical metrics such as majority voting, entropy, or other measures are used to validate the cluster assignment of a specific data point in the original dataset. Further details on the underlying principles of NEMI can be found in Sonnewald (2023), and the corresponding code is available on GitHub: https://github.com/CompClimate/NEMI.

https://doi.org/10.5194/egusphere-2026-1301
Preprint. Discussion started: 7 April 2026

For the NEMI method, as with many machine learning applications, data cleaning and pre-processing are crucial (Bishop and Nasrabadi, 2006). Pre-processing focuses on capturing covariance among variables rather than their individual magnitudes. For example, when analyzing the relationship between age and income, income values are typically much larger than age values, masking the influence of age factor unless putting both variables on comparable numerical ranges. From a machine learning perspective, proper pre-processing ensures that the data is more suitable for clustering analysis than the original unscaled data, as de Amorim et al. (2023) demonstrated, who emphasize the importance of appropriate scaling. The choice of scaling method depends on the nature of the input data, and significantly influences the clustering performance by either enhancing or obscuring the inherent data structure. In our case, we tested multiple scaling approaches and found that the quantile transformer yielded the most robust and consistent results. This method consistently outperformed others in terms of cluster separability and stability, indicating that it is particularly well suited for this study. The distributions of the original sea ice budget components are presented in Figure S6a. We observe that the dynamic component is skewed toward negative values (featured by coastal sea ice outward transport), the horizontal thermodynamic component is skewed toward positive values, and the vertical thermodynamic component exhibits two peaks near 0 and 0.0002 kg m^{-2} s^{-1}. We then applied a quantile transformer to scale the original data, transforming the data into normal distributions shown in Figure S6b. After scaling, the thermodynamic components are positively correlated with each other, while dynamics show a negative correlation with both thermodynamic components (Figure S6c-e). This suggests that in some areas (primarily coastal regions) where thermodynamic processes facilitate sea ice formation, dynamic processes act in the opposite way. In general, NEMI can now better identify relationships within a more balanced and normalized feature space.

3 Results

3.1 Climatological sea ice mass balance

Before determining regimes, we first provide a spatial overview of the thermodynamic and dynamic processes affecting sea ice. Figure 1 illustrates the geographical distributions of the climatological sea ice mass balance components during the growth seasons, both before and after scaling. To ensure that the subsequent clustering captures the covariance patterns of the components rather than being dominated by differences in their absolute magnitudes, we apply a quantile transformer to each field. This method standardizes the data by mapping each component to a normal distribution, improving comparability across variables. Notably, this scaling is only applied during the clustering process to group the model output in a way that highlights joint variability appropriately. For subsequent analyses of the physical interpretation, the data are projected back to their original physical units. The NEMO-SI³ model configuration used in this study has been evaluated against satellite observations and reanalysis datasets. It can effectively capture the main climatological features of Antarctic sea ice during the growth season and reproduces both the moderate increase before 2016 and the abrupt decline afterwards (Figure S4-S5), thus supporting its application in analyzing sea ice changes and associated mass balance components.

https://doi.org/10.5194/egusphere-2026-1301
Preprint. Discussion started: 7 April 2026

The original vertical thermodynamic component (Fig. 1a) displays an overall positive contribution to sea ice mass balance, particularly along the coast, with prominent high values in the Ross Sea and Weddell Sea. Note that a small fraction of values (5.5%) is negative and are omitted from the color bar for clarity. This gradient decreases towards lower latitudes, corresponding to the highest rates of new sea ice formation along the coast and in the polynya regions (Tamura et al., 2016; Nakata et al., 2021). After scaling (Fig. 1d), the coastal regions still display high values, while the ice edge regions are mapped to negative values. Most ice pack regions remain near zero.

Similarly, the original horizontal thermodynamic component (Fig. 1b) also shows a generally positive contribution to sea ice mass balance, albeit with slightly lower magnitudes than the vertical component. Higher values are observed in the southern Weddell Sea, southern Ross Sea and eastern Indian Ocean, while the other regions are close to zero. The scaled horizontal thermodynamics (Fig. 1e) exhibit a similar distribution to the scaled vertical component, but with greater variability, particularly in the western Pacific Ocean.

The original dynamic component (Fig. 1c) presents a negative contribution along the coast and positive for the rest. This suggests that dynamic processes such as advection and divergence transport sea ice away from the coast to lower latitudes, leading to higher vertical and horizontal thermodynamic processes along the coast (Fig. 1a-b). After scaling (Fig. 1f), these patterns become more distinct, with clearer positive contributions in the northern and western Weddell Sea, northern Ross Sea and East Antarctic.

Overall, the model's representation of climatological sea ice mass balance during the growth season aligns well with established understanding of thermodynamic and dynamic processes (Holland and Kwok, 2012; Haumann et al., 2016; Holland and Kimura, 2016; Himmich et al., 2023). Meanwhile, the scaling process highlights the spatial variance of each input rather than their individual magnitudes, providing a better foundation for applying the regime identification.

https://doi.org/10.5194/egusphere-2026-1301
Preprint. Discussion started: 7 April 2026

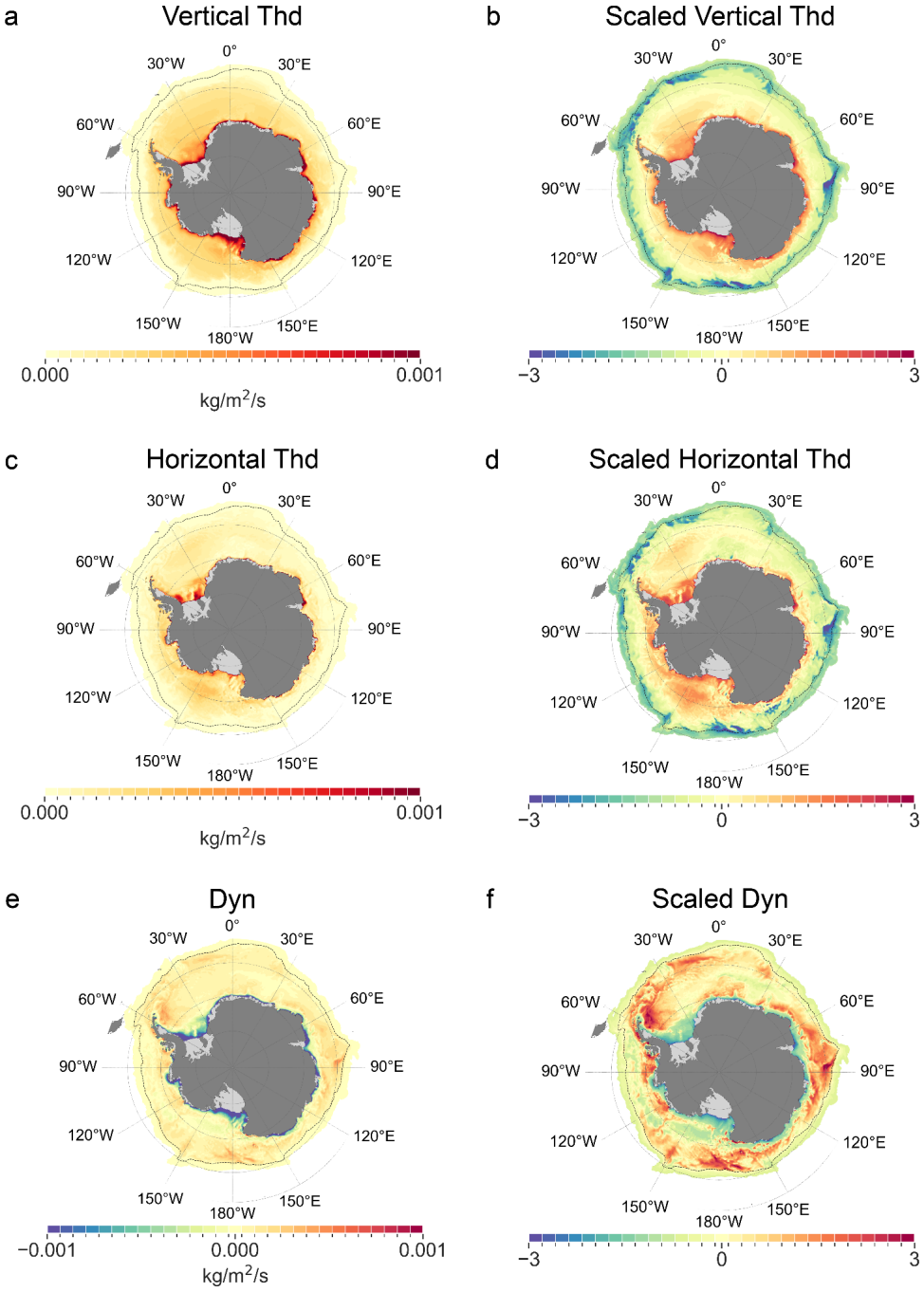

200

Figure 1: (a,c,e) Maps of the climatological (1981-2010) sea ice mass balance terms from model output during growth seasons (March to September), including vertical thermodynamics (bottom growth, bottom melt, snow-ice growth, surface melt), horizontal thermodynamics (lateral growth, lateral melt) and dynamics (sea ice transport, mechanical redistribution). (b,d,f) Same as (a,c,e) but scaled with a quantile transformer. Black contours indicate the 15% sea ice concentration (SIC) threshold, representing the approximate sea ice edge.

https://doi.org/10.5194/egusphere-2026-1301
Preprint. Discussion started: 7 April 2026

3.2 Objectively determined sea ice regimes

We first analyze climatological sea ice regimes and then explore their interannual variability to understand the mechanisms driving recent changes. With the preprocessed climatological sea ice budget components, we analyze the covariance structure within the data to determine regimes as statistically significant groupings of term magnitudes (Fig. 2). As described above, this approach can be viewed as a machine learning-based empirical leading-order process analysis (Kaiser et al., 2022). The first step in NEMI is to construct a low-dimensional embedded representation, also known as the "latent space". This latent space acts like a compressed map of the original data, revealing hidden patterns and relationships that are difficult to detect in the raw input space. A manifold methodology UMAP (Uniform Manifold Approximation and Projection) (Healy and McInnes, 2024) is employed for nonlinear dimensionality reduction and for strengthening associations between relevant structures in the data. The projection onto a lower-dimensional space is achieved by minimizing a cross-entropy cost function, which balances the preservation of local structures against the global covariance patterns in the original data. The UMAP parameters were chosen based on physical intuition and for the stability they offer to the embedding that facilitates robust clustering results, as confirmed by sensitivity tests showing minimal variation under different parameters. The embedding result (Fig. 3a) shows a covariance structure with distinct and well-separated shapes, indicating different regimes with specific characteristics.

Based on this visualization of the sea ice budget component relationship, we applied DBSCAN (Density-Based Spatial Clustering of Applications with Noise) (Ester et al., 1996) to cluster the well-separated shapes, a clustering method well-suited for identifying clusters with varying densities and nonlinear shapes. To improve the stability of the results, we conduct 100 iterations. The ensemble cluster results are then analyzed by assigning each point to a cluster based on the majority vote, i.e., the cluster label that appears most frequently for that point, across all iterations. Our clustering demonstrates strong stability, as evidenced by the extremely high probability of the final cluster being selected in 99% of ensemble members. As shown in Fig. 3b, DBSCAN successfully identified six distinct clusters corresponding to different sea ice regimes. Each data point represents a specific latitude-longitude location. A comparison with KMeans and Agglomerative clustering applied to the same embedding (Figure S7) further shows that DBSCAN more effectively captures the intrinsic structures, whereas the alternative methods either linearly split individual structures or merge partial regions into mixed clusters.

We project the six clusters identified back onto a geographical map to interpret their physical meaning (Fig. 3c). The six primary regimes are named based on their locations: Pack, Coast, OEdge (Outer Edge), IEdge (Inner Edge), WPO (Western Pacific Ocean), and Res (Residual). The corresponding area-averaged budget components are shown in Fig. 3d, with the spatial distribution shown in Figure S8. The 'Pack' regime, which covers the largest portion (52.6%), is located in the inner ice pack and dominated by first-year sea ice. It is characterized by consistent positive contributions from dynamics,

https://doi.org/10.5194/egusphere-2026-1301
Preprint. Discussion started: 7 April 2026

horizontal thermodynamics and vertical thermodynamics. This regime reflects directly that sea ice is expanding from summer to winter.

Using our framework, we can identify these divergence-dominated regions even where traditional geographic or empirical classifications would not distinguish them. The ‘Coast’ regime is mainly found along the coast, but also some offshore regions in the Indian Ocean, Ross Sea, Bellingshausen and Amundsen Seas, regions of prevalent sea ice divergence (Holland and Kimura, 2016). This regime is marked by significant negative dynamic contributions and positive thermodynamic contributions, indicating that sea ice is being transported away from those regions, while thermodynamics compensate for this loss. However, this does not necessarily reflect coastal processes such as landfast ice formation or coastal leads, but rather indicates divergence-dominated dynamics that may occur beyond the coastal zone.

‘OEdge’ and ‘IEdge’ are located at the outer and inner sea ice edge regions respectively and both are primarily dominated by dynamic processes. 'OEdge' experiences little horizontal formation, and is primarily shaped by dynamic processes and vertical thermodynamic melting, particularly in the Weddell Sea, Ross Sea, and eastern Indian Ocean (Figure S8g), likely due to direct exposure to the warmer lower-latitude ocean. Comparably, the ‘IEdge’ regime shows more moderate vertical thermodynamic loss and stronger horizontal thermodynamic growth, suggesting weaker melting than ‘OEdge’ due to the interior location of this regime. ‘WPO’ is a small but stably-identified regime, displaying positive vertical thermodynamics and positive dynamics in the western Pacific Ocean and parts of Eastern Antarctic. It is surrounded by the ‘Pack’ regime but stands out due to weaker horizontal thermodynamics. In this regime, sea ice convergence is exceptionally strong compared with other regimes and there is nearly no lateral growth. ‘Res’, the smallest regime (0.3%), is not discussed further due to its minimal spatial presence.

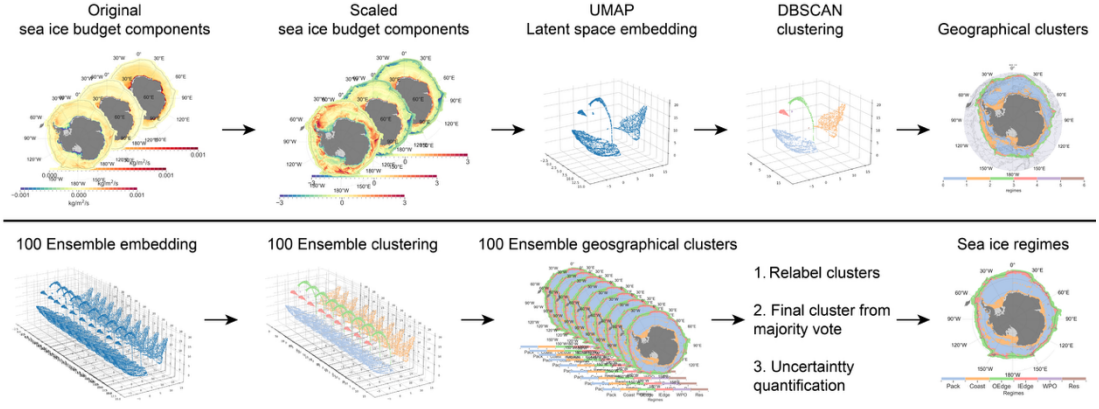

Figure 2: The upper row illustrates the transformation from raw data through scaling, embedding and clustering. The lower row shows the ensemble construction, cluster ranking and the final assignment of sea ice regime.

https://doi.org/10.5194/egusphere-2026-1301
Preprint. Discussion started: 7 April 2026

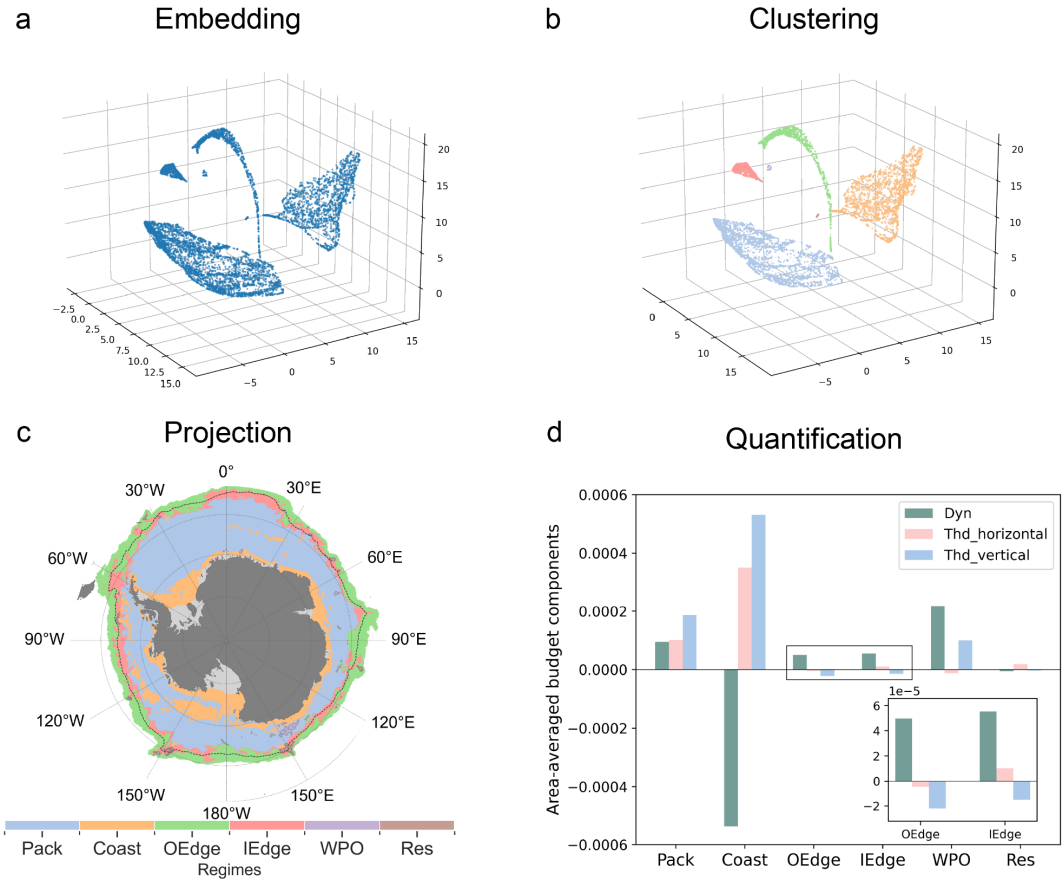

Figure 3: (a) UMAP embedding of the input data, illustrating the underlying structure. Note that the axes in the UMAP latent space are abstract and do not represent specific physical variables. (b) DBSCAN clustering applied on UMAP, identifying six clusters. (c) Projection of the clustered data onto the geographical map, highlighting spatial distribution. Black contour indicates the 15% SIC threshold, representing the approximate sea ice edge. (d) Area-averaged budget components (Unit: kg m^{-2} s^{-1}) for each regime, providing insights into cluster-specific characteristics. An inset zooms in on OEdge and IEdge regimes for better visibility.

3.3 Interannual variability of regimes

Moving beyond climatological averages, we now turn to the question of how each growth regime has evolved over time by applying the previous analysis (same processing steps and parameters) to annual model outputs from 1979 to 2023. For each year, the sea ice budget components during the growth season are clustered into six main regimes: 'Pack' 'Coast' 'OEdge', 'IEdge', 'WPO' and 'Res', with occasional minor regimes (<0.1% area) appearing, without any parameter tuning (see Supplementary Materials). These residuals are excluded to ensure consistency with the primary regimes identified in the climatological analysis. The minor regimes 'WPO' and 'Res', which together account for only 0.8% of the surface covered by sea ice in the clustering results, are excluded from the following discussion.

https://doi.org/10.5194/egusphere-2026-1301
Preprint. Discussion started: 7 April 2026

To assess how the identified regime areas vary over time, Figure 4 illustrates the percentages and anomalies of regime areas, alongside modeled SIE anomalies. Table 2 further provides trends in regime area for three periods (1979-2023, 1979-2015 and 2016-2023), as well as correlations between regime area anomalies and SIE anomalies. In agreement with observations (Figure S5b), the modeled SIE anomaly shows a weak positive trend before 2016 (0.11 million km^2 $decade^{-1}$), followed by a strong decline (-0.7 million km^2 $decade^{-1}$) after 2016, consistent with the onset of recent extreme sea ice loss.

Although all regimes exhibit interannual fluctuations in their spatial area, only the 'Coast' regime shows a statistically significant trend over the full period, with an average decrease of -0.11 million km^2 $decade^{-1}$. This decline is more pronounced in the post-2016 period (-0.21 million km^2 $decade^{-1}$). Compared with 1979-2015, the 'Coast' regime shows increased spatial extent west of the Antarctic Peninsula (Figure S9). The 'Pack' regime, which consistently accounts for the largest portion of the total sea ice area (47%–58%, Fig. 4a), mirrors the two-phase trend of the SIE anomaly. This dominant coverage reflects the prevailing pattern of sea ice advance during the growth season, which contributes to the 'Pack' regime's spatial persistence and temporal stability. The 'OEdge' and 'IEdge' regimes show insignificant decreasing trends prior to 2016, but 'IEdge' shows a sharp decline (-0.6 million km^2 $decade^{-1}$) after 2016.

Correlations between regime area anomalies and SIE anomalies further reveal that the 'Pack' regime interannual variations are closely tied to overall sea ice extent ($R = 0.47$). The 'Coast' regime is also positively correlated with SIE ($R = 0.41$), despite its decreasing long-term trend. In contrast, the 'OEdge' and 'IEdge' regimes show little correlation. Additionally, the significant anti-correlation between 'Pack' regime area and 'Coast' regime area ($r=-0.54$) indicates that an expansion of the 'Pack' regime coincides with a contraction of the 'Coast' regime. This relationship explains the relatively stable total area (73%-79%) occupied by these two regimes together over time (Fig. 4a).

These area variations are linked to different underlying dynamic (e.g., wind-driven divergence and advection) and thermodynamic (e.g., freezing and melting) processes (Figure S10; Table S1). For the 'Pack' regime, both dynamic and thermodynamic components weaken after 2016, suggesting that its post-2016 area decline is associated with an overall reduction in these key processes. In the 'Coast' regime, dynamic processes strengthen markedly after 2016 (0.66 kg m^{-2} s^{-1} $decade^{-1}$), while horizontal thermodynamic growth weakens (-0.58 kg m^{-2} s^{-1} $decade^{-1}$). This implies that increased divergence is no longer sufficiently compensated by thermodynamic gain, leading to the observed area decline. The 'OEdge' regime shows a significant decline before 2016, but no substantial trends afterward. The 'IEdge' regime shows weak and insignificant trends across all components. These contrasting variations reflect that regime area is controlled by the balance between thermodynamic and dynamic processes.

Figure 4 provides further insights into how each regime responded during recent sea ice extremes. In the 2017 growth season, when Antarctic SIE reached a record-low, the 'OEdge' and 'IEdge' regimes showed large negative area anomalies (Fig. 4b).

https://doi.org/10.5194/egusphere-2026-1301
Preprint. Discussion started: 7 April 2026

In the 2023 growth season, all regimes showed negative anomalies, with the 'Pack' regime contributing the largest deficit. Meanwhile, the spatial distribution of regimes differed a lot from previous years, particularly in the location of the 'Coast' regime (see Supplementary Materials). In addition, since our analysis is conducted on the growth season averages, many short-term processes (e.g., storms, heatwaves) may be obscured. To better understand the drivers of extreme sea ice loss, future applications of this framework could consider monthly or even finer temporal resolutions. This would allow for a more detailed investigation of specific processes affecting sea ice variability, which lies beyond the scope of the present study.

Table 2. Trends (10^6 km^2 decade^{-1}) of areas occupied by each regime and SIE anomaly for 1979-2023, 1979-2015 and 2016-2023, and correlations of regime area anomalies with SIE anomalies. Bold indicates significance at 95% confidence.

	Trend (1979-2023)	Trend (1979-2015)	Trend (2016-2023)	Corr(Area_ano, SIE_ano)
SIE anomaly	-0.05	**0.11**	-0.7	\
Pack	0.07	0.13	-0.3	**0.47**
Coast	**-0.11**	-0.04	-0.21	**0.41**
OEdge	-0.06	-0.02	-0.27	0.17
IEdge	-0.03	-0.02	**-0.6**	0.27

https://doi.org/10.5194/egusphere-2026-1301
Preprint. Discussion started: 7 April 2026

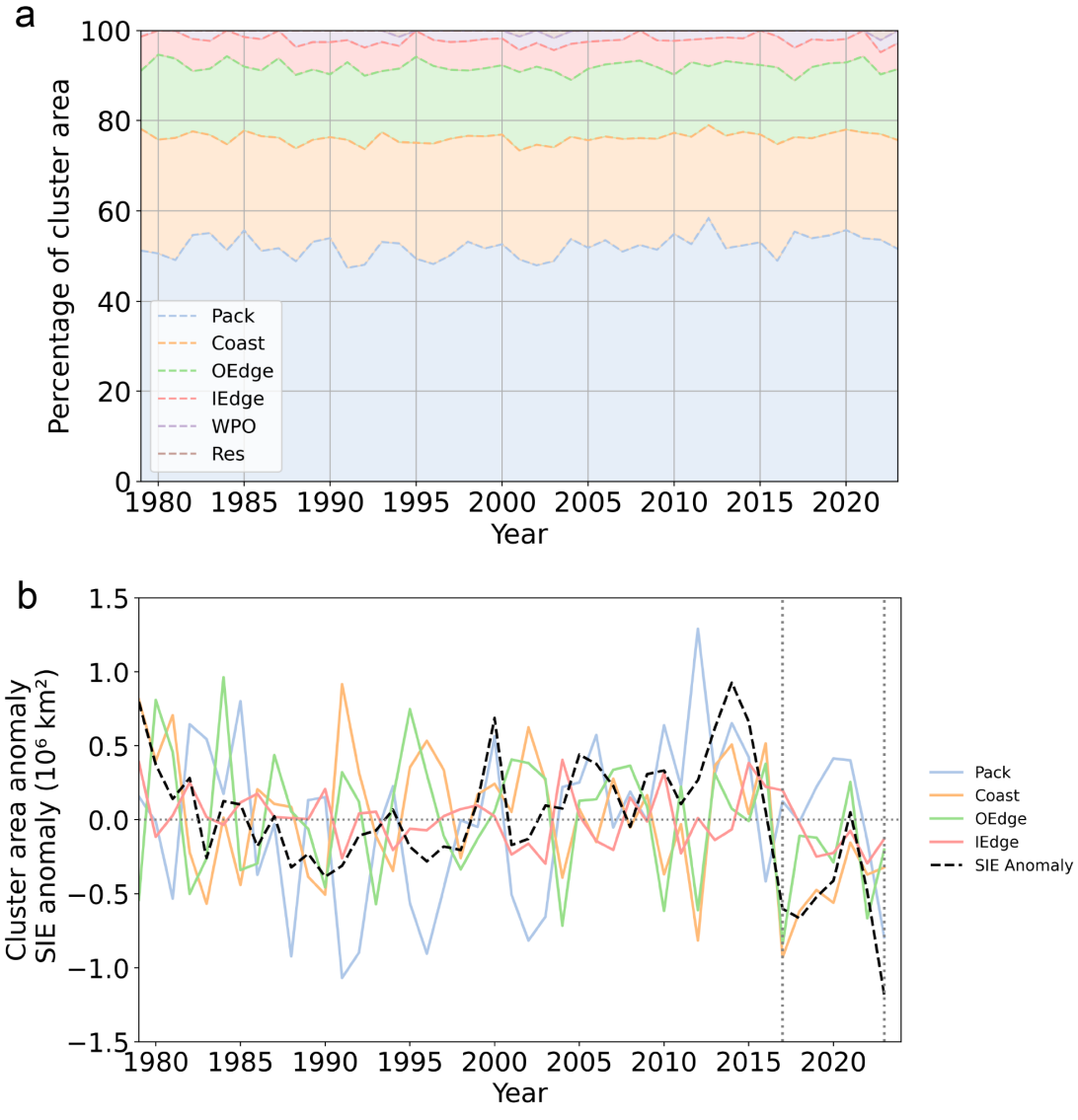

Figure 4: (a) Stacked time series of percentage of regime areas for 'Pack', 'Coast', 'OEdge', 'IEdge', 'WPO' and 'Res' from 1979 to 2023. (b) Area anomalies (Unit: 10^6 km^2) for 'Pack', 'Coast', 'OEdge', and 'IEdge' regimes, along with sea ice extent (SIE) anomalies from the model, averaged over the growth season (March–September). Extreme years including 2017 and 2023 are indicated with vertical lines.

4 Discussion

In this study, we developed an objective framework to identify the dominant physical processes governing Antarctic sea ice variability, looking at time mean and interannual variability data from 1979 to 2023. We focused particularly on shifts between the pre- and post-2016 periods, when Antarctic sea ice shifted from net-growth to net-loss, and we revealed that this

https://doi.org/10.5194/egusphere-2026-1301
Preprint. Discussion started: 7 April 2026

change was primarily related with significant area loss in the coastal regime and the pack ice regime, reflecting the combined effects of dynamic and thermodynamic processes.

Our framework is based on the Antarctic sea ice budget components (vertical thermodynamics, horizontal thermodynamics and dynamics) using an ascendant machine-learning-based NEMI workflow. We objectively identified six distinct regimes in the climatological data. The 'Pack' regime is located in the inner ice pack region, characterized by consistent sea ice growth driven by both thermodynamic and dynamic processes. The 'Coast' regime, along the coast of the continent and offshore regions of the Amundsen-Bellingshausen and Ross Seas, features strong dynamic divergence that is compensated by thermodynamic growth. The 'OEdge' and 'IEdge' regimes represent sea ice edge processes but with different horizontal thermodynamics behaviors. The 'WPO' regime usually occurs in the western Pacific Ocean, while the 'Res' regime is a minimal regime with limited impact. From 1979 to 2023, only the 'Coast' regime showed a significant decreasing trend (-0.11 million km² decade^{-1}), particularly accelerating after 2016. Correlation analyses further revealed that changes in 'Pack' and 'Coast' regime areas are closely linked to SIE anomalies, suggesting their critical roles in Antarctic sea ice variability. These regime area changes were accompanied by distinct shifts in dynamic and thermodynamic drivers. Although seasonal averaging may obscure short-term but critical processes such as strong storms, atmospheric heat intrusions, or regional ocean heat intrusions, the framework demonstrates the potential for deeper investigation into process-based drivers of sea ice change.

These changes in regime areas have broader implications. For instance, the shrinking of the 'Coast' regime may indicate a weakening of new ice formation in coastal polynya, which play key roles in brine rejection and Antarctic Bottom Water formation, potentially influencing Southern Ocean overturning circulation. Meanwhile, reductions in the 'Pack' regimes may indicate a loss of thick compacted ice, decreasing the sea ice system's resilience to anomalous atmospheric and oceanic forcing. Overall, such shifts in the spatial distribution of sea ice regimes are likely to modify the timing of seasonal advance or retreat, with further impacts on the broader climate system.

This process-based approach has several advantages. First, it identifies regimes characterized by distinct combinations of underlying processes without relying on prior assumptions, thus complementing existing geographic or empirical classifications and enabling a more mechanistic understanding of sea ice variability. Although simple threshold-based classifications derived from SIC or bathymetry (as shown in Figure S11) can reproduce circumpolar patterns that may appear similar to the climatological regimes identified by NEMI (Fig. 3c), substantial discrepancies emerge at the monthly scale (comparing Figure S1 and Figure S11). This difference reflects the additional process-wise information contained in the NEMI framework, where thermodynamic and dynamic contributions are jointly considered, while a criterion based on SIC or bathymetry alone can combine regions governed by different dynamic regimes. Second, the framework captures the temporal evolution of these regimes over the past decades, allowing regime shifts or area changes to be linked with external

https://doi.org/10.5194/egusphere-2026-1301
Preprint. Discussion started: 7 April 2026

forcing such as wind, temperature, or large-scale circulation anomalies. Such year-to-year shifts can only be captured by a process-based regime identification framework, rather than by fixed SIC or bathymetry criteria (Figure S11). Third, we reveal underappreciated features that would likely be missed in traditional frameworks. For example, the identification of "Coast" regimes exhibiting coastal-like characteristics in areas not directly adjacent to the Antarctic continent. Fourth, the method is flexible in its application across temporal scales (from synoptic events to decadal trends), spatial resolutions, and a variety of input datasets (e.g., thermodynamic fluxes, wind stress, oceanic heat transport), depending on the scientific objective. It can be further extended to incorporate marginal ice zone dynamics governed by wave–ice interactions, landfast ice, or coastal polynya processes, potentially enabling the identification of more localized or process-specific regimes. Finally, our physically based regime framework provides an application to Antarctic sea ice, and complements broader efforts across Earth system science to detect and interpret process-based regime transitions.

This study presents the first application of the NEMI workflow to Antarctic sea ice budget components, providing a process-based perspective to objectively define sea ice regimes and explore the mechanisms driving Antarctic sea ice changes. While the current regime identification provides a valuable framework based on thermodynamic and dynamic mass balance components, it also highlights opportunities for the next phase of research. In particular, coastal processes (e.g., landfast ice formation, shear zones) and marginal ice zone dynamics influenced by wave–ice interactions are not explicitly resolved in the current approach. This is primarily because the input fields are limited to large-scale thermodynamic and dynamic terms. Future work could incorporate additional model diagnostics or external datasets (e.g., sea ice deformation, wave-related parameters) to capture finer-scale processes and identify more physically detailed sea ice regimes. Moreover, regional assessments that go beyond changes in regime area (e.g., shifts in intensity and location) will be critical for identifying potential regime transitions and improving our physical understanding of Antarctic sea ice variability. Together, these approaches will help us better understand how sea ice behaves and its impact on the wider Southern Ocean.

Code and data availability

All data are available in the main text or the supplementary materials. NSIDC sea ice concentration data are available at https://nsidc.org/data/nsidc-0051/versions/2 with near-real-time data at https://nsidc.org/data/nsidc-0081/versions/2. The GIOMAS SIT reanalysis data are available at http://psc.apl.washington.edu/zhang/Global_seaice/data.html. The scripts used to produce the figures in this paper are archived in Zenodo (DOI: https://doi.org/10.5281/zenodo.14495814).

Author contributions

Conceptualization: FM, HG, MS, QY; Methodology: MS; Investigation: JW, NP; Visualization: JW, NP; Supervision: FM, HG, MS, QY, DC; Writing—original draft: JW; Writing—review & editing: All authors.

https://doi.org/10.5194/egusphere-2026-1301
Preprint. Discussion started: 7 April 2026

Competing interests

At least one of the (co-)authors is a member of the editorial board of The Cryosphere.

Acknowledgements

This study was funded by the National Natural Science Foundation of China (Nos. 42530406, 41941009), and Program of China Scholarship Council (No. 202206380090). This work has received support from the Belgian Science Policy (BELSPO) project RESIST ("Recent Arctic and Antarctic sea ice lows: same causes, same impacts? »)

References

de Amorim, L. B., Cavalcanti, G. D., and Cruz, R. M.: The choice of scaling technique matters for classification performance, Applied Soft Computing, 133, 109924, 2023.

Ayres, H. C., Screen, J. A., Blockley, E. W., and Bracegirdle, T. J.: The Coupled Atmosphere–Ocean Response to Antarctic Sea Ice Loss, Journal of Climate, 35, 4665–4685, https://doi.org/10.1175/JCLI-D-21-0918.1, 2022.

Bishop, C. M. and Nasrabadi, N. M.: Pattern recognition and machine learning, Springer, 2006.

Comiso, J. C., Gersten, R. A., Stock, L. V., Turner, J., Perez, G. J., and Cho, K.: Positive Trend in the Antarctic Sea Ice Cover and Associated Changes in Surface Temperature, Journal of Climate, 30, 2251–2267, https://doi.org/10.1175/JCLI-D-16-0408.1, 2017.

Day, N. S., Bennetts, L. G., O'Farrell, S. P., Alberello, A., and Montiel, F.: Analysis of the Antarctic Marginal Ice Zone Based on Unsupervised Classification of Standalone Sea Ice Model Data, JGR Oceans, 129, e2024JC020953, https://doi.org/10.1029/2024JC020953, 2024.

DiGirolamo, N., Parkinson, C., Cavalieri, D., Gloersen, P., and Zwally, H.: Sea Ice Concentrations from Nimbus-7 SMMR and DMSP SSM/I-SSMIS Passive Microwave Data, Version 2, https://doi.org/10.5067/MPYG15WAA4WX, 2022.

Eayrs, C., Holland, D., Francis, D., Wagner, T., Kumar, R., and Li, X.: Understanding the Seasonal Cycle of Antarctic Sea Ice Extent in the Context of Longer-Term Variability, Reviews of Geophysics, 57, 1037–1064, https://doi.org/10.1029/2018RG000631, 2019.

Espinosa, Z. I., Blanchard-Wrigglesworth, E., and Bitz, C. M.: Understanding the drivers and predictability of record low Antarctic sea ice in austral winter 2023, Commun Earth Environ, 5, 723, https://doi.org/10.1038/s43247-024-01772-2, 2024.

Ester, M., Kriegel, H.-P., Sander, J., and Xu, X.: A density-based algorithm for discovering clusters in large spatial databases with noise, in: Proceedings of the Second International Conference on Knowledge Discovery and Data Mining, Portland, Oregon, 226–231, 1996.

Goosse, H., Allende Contador, S., Bitz, C. M., Blanchard-Wrigglesworth, E., Eayrs, C., Fichefet, T., Himmich, K., Huot, P.-V., Klein, F., Marchi, S., Massonnet, F., Mezzina, B., Pelletier, C., Roach, L., Vancoppenolle, M., and Van Lipzig, N. P. M.: Modulation of the seasonal cycle of the Antarctic sea ice extent by sea ice processes and feedbacks with the ocean and the atmosphere, The Cryosphere, 17, 407–425, https://doi.org/10.5194/tc-17-407-2023, 2023.

https://doi.org/10.5194/egusphere-2026-1301
Preprint. Discussion started: 7 April 2026

Haumann, F. A., Gruber, N., Münnich, M., Frenger, I., and Kern, S.: Sea-ice transport driving Southern Ocean salinity and its recent trends, Nature, 537, 89–92, https://doi.org/10.1038/nature19101, 2016.

Healy, J. and McInnes, L.: Uniform manifold approximation and projection, Nat Rev Methods Primers, 4, 82, https://doi.org/10.1038/s43586-024-00363-x, 2024.

Hersbach, H., Bell, B., Berrisford, P., Hirahara, S., Horányi, A., Muñoz-Sabater, J., Nicolas, J., Peubey, C., Radu, R., Schepers, D., Simmons, A., Soci, C., Abdalla, S., Abellan, X., Balsamo, G., Bechtold, P., Biavati, G., Bidlot, J., Bonavita, M., Chiara, G., Dahlgren, P., Dee, D., Diamantakis, M., Dragani, R., Flemming, J., Forbes, R., Fuentes, M., Geer, A., Haimberger, L., Healy, S., Hogan, R. J., Hólm, E., Janisková, M., Keeley, S., Laloyaux, P., Lopez, P., Lupu, C., Radnoti, G., Rosnay, P., Rozum, I., Vamborg, F., Villaume, S., and Thépaut, J.: The ERA5 global reanalysis, Q.J.R. Meteorol. Soc., 146, 1999–2049, https://doi.org/10.1002/qj.3803, 2020.

Himmich, K., Vancoppenolle, M., Madec, G., Sallée, J.-B., Holland, P. R., and Lebrun, M.: Drivers of Antarctic sea ice advance, Nat Commun, 14, 6219, https://doi.org/10.1038/s41467-023-41962-8, 2023.

Himmich, K., Vancoppenolle, M., Stammerjohn, S., Bocquet, M., Madec, G., Sallée, J., and Fleury, S.: Thermodynamics Drive Post-2016 Changes in the Antarctic Sea Ice Seasonal Cycle, JGR Oceans, 129, e2024JC021112, https://doi.org/10.1029/2024JC021112, 2024.

Hobbs, W., Spence, P., Meyer, A., Schroeter, S., Fraser, A. D., Reid, P., Tian, T. R., Wang, Z., Liniger, G., Doddridge, E. W., and Boyd, P. W.: Observational Evidence for a Regime Shift in Summer Antarctic Sea Ice, Journal of Climate, https://doi.org/10.1175/JCLI-D-23-0479.1, 2024.

Holland, P. R. and Kimura, N.: Observed Concentration Budgets of Arctic and Antarctic Sea Ice, Journal of Climate, 29, 5241–5249, https://doi.org/10.1175/JCLI-D-16-0121.1, 2016.

Holland, P. R. and Kwok, R.: Wind-driven trends in Antarctic sea-ice drift, Nature Geosci, 5, 872–875, https://doi.org/10.1038/ngeo1627, 2012.

Jena, B., Kshitija, S., Bajish, C. C., Turner, J., Holmes, C., Wilkinson, J., Mohan, R., and Thamban, M.: Evolution of Antarctic Sea Ice Ahead of the Record Low Annual Maximum Extent in September 2023, Geophysical Research Letters, 51, e2023GL107561, https://doi.org/10.1029/2023GL107561, 2024.

Jenniges, Y., Sonnewald, M., Maneth, S., Olsen, A., and Koch, B. P.: Unveiling 3D ocean biogeochemical provinces in the North Atlantic: A systematic comparison and validation of clustering methods, Ecological Informatics, 91, 103390, https://doi.org/10.1016/j.ecoinf.2025.103390, 2025.

Kaiser, B. E., Saenz, J. A., Sonnewald, M., and Livescu, D.: Automated identification of dominant physical processes, Engineering Applications of Artificial Intelligence, 116, 105496, https://doi.org/10.1016/j.engappai.2022.105496, 2022.

Kusahara, K., Tatebe, H., Hajima, T., Saito, F., and Kawamiya, M.: Antarctic Sea Ice Holds the Fate of Antarctic Ice-Shelf Basal Melting in a Warming Climate, Journal of Climate, 36, 713–743, https://doi.org/10.1175/JCLI-D-22-0079.1, 2023.

Li, Q., England, M. H., Hogg, A. McC., Rintoul, S. R., and Morrison, A. K.: Abyssal ocean overturning slowdown and warming driven by Antarctic meltwater, Nature, 615, 841–847, https://doi.org/10.1038/s41586-023-05762-w, 2023.

Lim, S. M., van Dijken, G. L., and Arrigo, K. R.: Spatial and Interannual Variability of Antarctic Sea Ice Bottom Algal Habitat, 2004–2019, Journal of Geophysical Research: Oceans, 128, e2023JC020055, https://doi.org/10.1029/2023JC020055, 2023.

https://doi.org/10.5194/egusphere-2026-1301
Preprint. Discussion started: 7 April 2026

Liu, J., Curry, J. A., and Martinson, D. G.: Interpretation of recent Antarctic sea ice variability, Geophysical Research Letters, 31, 2003GL018732, https://doi.org/10.1029/2003GL018732, 2004.

Locarnini, M., Mishonov, A., Baranova, O., Boyer, T., Zweng, M., Garcia, H., Reagan, J., Seidov, D., Weathers, K., Paver, C., Smolyar, I., Baranova, O., Boyer, T., Zweng, M., Garcia, H., Reagan, J., Seidov, D., Weathers, K., Paver, C., and Smolyar, I.: World Ocean Atlas 2018, Volume 1: Temperature, 2018.

Madec, G., Bell, M., Benshila, R., Blaker, A., Boudrallé-Badie, R., Bricaud, C., Bruciaferri, D., Carneiro, D., Castrillo, M., Calvert, D., Chanut, J., Clementi, E., Coward, A., Lavergne, C. de, Dobricic, S., Epicoco, I., Éthé, C., Fiedler, E., Ford, D., Furner, R., Ganderton, J., Graham, T., Harle, J., Hutchinson, K., Iovino, D., King, R., Lea, D., Levy, C., Lovato, T., Maisonnave, E., Mak, J., Sanchez, J. M. C., Martin, M., Martin, N., Martins, D., Masson, S., Mathiot, P., Mele, F., Mocavero, S., Moulin, A., Müller, S., Nurser, G., Oddo, P., Paronuzzi, S., Paul, J., Peltier, M., Person, R., Rousset, C., Rynders, S., Samson, G., Schroeder, D., Storkey, D., Storto, A., Téchené, S., Vancoppenolle, M., and Wilson, C.: NEMO Ocean Engine Reference Manual 5.0, https://doi.org/10.5281/zenodo.14515373, 2024.

Massom, R. A., Scambos, T. A., Bennetts, L. G., Reid, P., Squire, V. A., and Stammerjohn, S. E.: Antarctic ice shelf disintegration triggered by sea ice loss and ocean swell, Nature, 558, 383–389, https://doi.org/10.1038/s41586-018-0212-1, 2018.

Meehl, G. A., Arblaster, J. M., Chung, C. T. Y., Holland, M. M., DuVivier, A., Thompson, L., Yang, D., and Bitz, C. M.: Sustained ocean changes contributed to sudden Antarctic sea ice retreat in late 2016, Nat Commun, 10, 14, https://doi.org/10.1038/s41467-018-07865-9, 2019.

Nakata, K., Ohshima, K. I., and Nihashi, S.: Mapping of Active Frazil for Antarctic Coastal Polynyas, With an Estimation of Sea-Ice Production, Geophysical Research Letters, 48, e2020GL091353, https://doi.org/10.1029/2020GL091353, 2021.

Parkinson, C. L.: A 40-y record reveals gradual Antarctic sea ice increases followed by decreases at rates far exceeding the rates seen in the Arctic, Proc. Natl. Acad. Sci. U.S.A., 116, 14414–14423, https://doi.org/10.1073/pnas.1906556116, 2019.

Pirlet, N., Fichefet, T., Vancoppenolle, M., Fraser, A. D., Mathiot, P., Rousset, C., Barthélemy, A., Barriat, P.-Y., Pelletier, C., Madec, G., and Kittel, C.: Benefits of a Landfast Ice Representation on Simulated Antarctic Sea Ice and Coastal Polynya Dynamics, Journal of Geophysical Research: Oceans, 130, e2024JC022032, https://doi.org/10.1029/2024JC022032, 2025.

Purich, A. and Doddridge, E. W.: Record low Antarctic sea ice coverage indicates a new sea ice state, Commun Earth Environ, 4, 314, https://doi.org/10.1038/s43247-023-00961-9, 2023.

Raphael, M. N. and Handcock, M. S.: A new record minimum for Antarctic sea ice, Nat Rev Earth Environ, 3, 215–216, https://doi.org/10.1038/s43017-022-00281-0, 2022.

Raphael, M. N. and Hobbs, W.: The influence of the large-scale atmospheric circulation on Antarctic sea ice during ice advance and retreat seasons, Geophysical Research Letters, 41, 5037–5045, https://doi.org/10.1002/2014GL060365, 2014.

Rousset, C., Vancoppenolle, M., Madec, G., Fichefet, T., Flavoni, S., Barthélemy, A., Benshila, R., Chanut, J., Levy, C., Masson, S., and Vivier, F.: The Louvain-La-Neuve sea ice model LIM3.6: global and regional capabilities, Geoscientific Model Development, 8, 2991–3005, https://doi.org/10.5194/gmd-8-2991-2015, 2015.

Schroeter, S., O'Kane, T. J., and Sandery, P. A.: Antarctic sea ice regime shift associated with decreasing zonal symmetry in the Southern Annular Mode, The Cryosphere, 17, 701–717, https://doi.org/10.5194/tc-17-701-2023, 2023.

https://doi.org/10.5194/egusphere-2026-1301
Preprint. Discussion started: 7 April 2026

Sohail, T. and Zika, J. D.: Unsupervised Classification Identifies Warm, Fresh, and Dense Regimes of the Antarctic Margins, Journal of Physical Oceanography, 54, 1229–1242, https://doi.org/10.1175/JPO-D-23-0153.1, 2024.

Sonnewald, M.: A hierarchical ensemble manifold methodology for new knowledge on spatial data: An application to ocean physics, https://doi.org/10.22541/essoar.168056792.25480169/v1, 4 April 2023.

Sonnewald, M., Reeve, K. A., and Lguensat, R.: A Southern Ocean supergyre as a unifying dynamical framework identified by physics-informed machine learning, Commun Earth Environ, 4, 153, https://doi.org/10.1038/s43247-023-00793-7, 2023.

Søren, R., Bendtsen, J., Delille, B., Dieckmann, G. S., Glud, R. N., Kennedy, H., Mortensen, J., Papadimitriou, S., Thomas, D. N., and Tison, J.-L.: Sea ice contribution to the air–sea CO_2 exchange in the Arctic and Southern Oceans, Tellus B: Chemical and Physical Meteorology, 63, 823–830, https://doi.org/10.1111/j.1600-0889.2011.00571.x, 2011.

Swadling, K. M., Constable, A. J., Fraser, A. D., Massom, R. A., Borup, M. D., Ghigliotti, L., Granata, A., Guglielmo, L., Johnston, N. M., Kawaguchi, S., Kennedy, F., Kiko, R., Koubbi, P., Makabe, R., Martin, A., McMinn, A., Moteki, M., Pakhomov, E. A., Peeken, I., Reimer, J., Reid, P., Ryan, K. G., Vacchi, M., Virtue, P., Weldrick, C. K., Wongpan, P., and Wotherspoon, S. J.: Biological responses to change in Antarctic sea ice habitats, Frontiers in Ecology and Evolution, 10, https://doi.org/10.3389/fevo.2022.1073823, 2023.

Tamura, T., Ohshima, K. I., Fraser, A. D., and Williams, G. D.: Sea ice production variability in Antarctic coastal polynyas, Journal of Geophysical Research: Oceans, 121, 2967–2979, https://doi.org/10.1002/2015JC011537, 2016.

Turner, J. and Comiso, J.: Solve Antarctica's sea-ice puzzle, Nature, 547, 275–277, https://doi.org/10.1038/547275a, 2017.

Wachter, P., Reiser, F., Friedl, P., and Jacobeit, J.: A new approach to classification of 40 years of Antarctic sea ice concentration data, Intl Journal of Climatology, 41, https://doi.org/10.1002/joc.6874, 2021.

Wang, J., Luo, H., Yang, Q., Liu, J., Yu, L., Shi, Q., and Han, B.: An Unprecedented Record Low Antarctic Sea-ice Extent during Austral Summer 2022, Advances in Atmospheric Sciences, https://doi.org/10.1007/s00376-022-2087-1, 2022.

Wang, J., Massonnet, F., Goosse, H., Luo, H., Barthélemy, A., and Yang, Q.: Synergistic atmosphere-ocean-ice influences have driven the 2023 all-time Antarctic sea-ice record low, Commun Earth Environ, 5, 415, https://doi.org/10.1038/s43247-024-01523-3, 2024.

van Westen, R. M., Jacques-Dumas, V., Boot, A. A., and Dijkstra, H. A.: The Role of Sea Ice Insulation Effects on the Probability of AMOC Transitions, Journal of Climate, https://doi.org/10.1175/JCLI-D-24-0060.1, 2024.

Zhang, J. and Rothrock, D. A.: Modeling Global Sea Ice with a Thickness and Enthalpy Distribution Model in Generalized Curvilinear Coordinates, Monthly Weather Review, 131, 845–861, https://doi.org/10.1175/1520-0493(2003)131%253C0845:MGSIWA%253E2.0.CO;2, 2003.

Zhang, L., Delworth, T. L., Yang, X., Zeng, F., Lu, F., Morioka, Y., and Bushuk, M.: The relative role of the subsurface Southern Ocean in driving negative Antarctic Sea ice extent anomalies in 2016–2021, Commun Earth Environ, 3, 302, https://doi.org/10.1038/s43247-022-00624-1, 2022.

Zuo, H., Balmaseda, M. A., Tietsche, S., Mogensen, K., and Mayer, M.: The ECMWF operational ensemble reanalysis–analysis system for ocean and sea ice: a description of the system and assessment, Ocean Science, 15, 779–808, https://doi.org/10.5194/os-15-779-2019, 2019.

https://doi.org/10.5194/egusphere-2026-1301
Preprint. Discussion started: 7 April 2026

Zweng, M., Reagan, J., Seidov, D., Boyer, T., Locarnini, M., Garcia, H., Mishonov, A., Baranova, O., Weathers, K., Paver, C., Smolyar, I., Seidov, D., Boyer, T., Locarnini, M., Garcia, H., Mishonov, A., Baranova, O., Weathers, K., Paver, C., and
535 Smolyar, I.: World Ocean Atlas 2018, Volume 2: Salinity, 2019.